Transverse lattice calculation of the pion light-cone wave functions

Simon Dalley
Department of Physics, University of Wales Swansea, Singleton Park, Swansea SA2 8PP, United Kingdom

Brett van de Sande
Geneva College, 3200 College Avenue, Beaver Falls, Pennsylvania 15010, USA

(Received 7 February 2003; published 24 June 2003)

We calculate the light-cone wave functions of mesons by solving their bound state problem in a coarse transverse lattice gauge theory using discrete light cone quantization. A large-N_c approximation is made and the light-cone Hamiltonian expanded in massive dynamical fields at fixed lattice spacing. In contrast with earlier calculations, we include contributions from states containing many gluonic link fields between the quarks. The Hamiltonian is renormalized by a combination of covariance conditions on bound states and fitting the physical masses $\mathcal{M}_\rho$ and $\mathcal{M}_\pi$, decay constant f_π, and the string tension $\sqrt{\sigma}$. Good covariance is obtained for the lightest 0^{-+} state, which we compare with the pion. Many observables can be deduced from its light-cone wave functions. After perturbative evolution, the quark valence structure function is found to be consistent with the experimental pion structure function deduced from Drell-Yan pi-nucleon data in the valence region $x>0.5$. In addition, the distribution amplitude is consistent with the experimental pion distribution deduced from the $\pi\gamma^*\gamma$ transition form factor and diffractive dissociation. A new observable we calculate is the probability for quark helicity correlation. We predict a 45% probability that the valence-quark helicities are aligned in the pion.

DOI: 10.1103/PhysRevD.67.114507 PACS number(s): 11.15.Ha, 12.38.Gc

I. INTRODUCTION

Light-cone wave functions encode all of the bound state quark and gluonic properties of hadrons, including their momentum, spin and flavor correlations, in the form of universal process- and frame-independent amplitudes (see, for example, Ref. [1]). Hadronic observables represented as matrix elements of currents are easily expressed in terms of overlaps of light-cone wave functions. To compute the wave functions, one must diagonalize the light-cone Hamiltonian of QCD in a Fock space of quark and gluonic degrees of freedom. A promising method to achieve this is the transverse lattice formulation of gauge theory [2,3]. In this approach, the physical gluonic degrees of freedom are represented by gauge-covariant links of color flux on a lattice transverse to the null plane of quantization. In this paper, we set up the method and solve for the light-cone wave functions of light mesons using a physically realistic truncation of Fock space on a coarse lattice, spacing $\sim 2/3$ fm. We obtain good covariance for the light-cone wave function of the lightest meson, which we identify with the pion. Results for the pion distribution amplitude (valence quark wave function at small transverse separation) and distribution function (valence quark probability at any transverse separation) are consistent with the most recent experimental results in the valence region of light-cone momenta. We find the distribution amplitude to be

$$\phi_\pi(x)=6x(1-x)\{1+0.15(2)C_2^{3/2}(1-2x)+0.04(1)C_4^{3/2}(1-2x)\}, \tag{1}$$

while the distribution function is

$$V_\pi(x)=\frac{(1-x)^{0.33(2)}}{x^{0.7(1)}}\{0.33(3)-1.1(2)\sqrt{x}+2.0(3)x\}. \tag{2}$$

where x is the quark light-cone momentum fraction carried in the pion. The transverse renormalization scale should be 0.5 GeV if the first moment of V_π is to agree with experiment. As a further application of the light-cone wave functions, we also compute the probability for a valence quark of momentum fraction x to have its helicity correlated with that of the anti-quark in the pion. We find surprisingly a large probability $\sim 45\%$ for the quark and anti-quark helicities to be aligned, even though the pion spin is 0. These represent our main results.

Attempts to solve transverse lattice QCD have been renewed in recent years for both the pure gauge theory [4–6] and mesons [7–9]. The most succesful approaches have employed the original idea [2] of a $1/N_c$ and color-dielectric expansion in dynamical fields to approximate the light-cone QCD Hamiltonian on a coarse transverse lattice. For pure gauge theory, to lowest non-trivial order of the expansion, requirements of vacuum stability, Lorentz and gauge invariance alone were found to constrain the coarse lattice Hamiltonian sufficiently accurately for first-principles predictions of the glueball states [5]. Extension of this work to light mesons introduced quarks and imposed a (Tamm-Dancoff) restriction on the number of link fields in Fock space [7]. In previous calculations [8,9], not more than one link field was allowed in a meson. This effectively restricts the transverse size to $<2/3$ fm, which is unrealistic for light mesons. In this case, the correct Hamiltonian could not be accurately identified using Lorentz and gauge invariance alone. Some phenomenology was also needed.

 ©2003 The American Physical Society

In this paper, we again use the lowest non-trivial order of the color-dielectric expansion of the Hamiltonian, but relax the Tamm-Dancoff cutoff on the space of states. This allows light mesons to expand to their physical transverse size. It also means that one begins to take account of the full pure-glue dynamics in the meson sector. While the results are now realistic, we find that it is still necessary to use some phenomenological fitting of masses and decay constants, in addition to optimizing Lorentz covariance, to obtain unambiguous couplings in the coarse-lattice Hamiltonian. We believe this is due to the absence, in the currently employed transverse lattice Hamiltonian, of operators needed to optimize chiral symmetry. We show that such operators would occur at higher order of the color-dielectric expansion. In the next section, we review and extend the previous work. Section III describes the procedure we employ for fixing the various couplings that appear in the Hamiltonian. Finally, our results for pion observables are discussed in Sec. IV. Chiral symmetry issues are discussed in the Appendix.

II. TRANSVERSE LATTICE MESONS

A. Hamiltonian

We introduce continuum light-cone coordinates $x^{\pm}=(x^0 \pm x^3)/\sqrt{2}$ and discretize the transverse coordinates $\mathbf{x}=(x^1,x^2)$ on a square lattice of spacing a. Lorentz indices μ,ν are split into light-cone indices $\alpha,\beta\in\{+,-\}$ and transverse indices $r,s\in\{1,2\}$. Subsequent analysis is done to leading order of the $1/N_c$ expansion of the gauge group $SU(N_c)$. Quark fields $\Psi(x^+,x^-,\mathbf{x})$ in the fundamental representation and gauge potentials $A_\alpha(x^+,x^-,\mathbf{x})$ in the adjoint representation of $SU(N_c)$ are associated to the sites of the transverse lattice. Link fields $M_r(x^+,x^-,\mathbf{x})$, which we choose to be complex $N_c\times N_c$ matrices, are associated with the directed link from $\mathbf{x}$ to $\mathbf{x}+a\hat{\mathbf{r}}$. They carry flux from site to site. This use of disordered link variables implies that a coarse transverse lattice is being considered.

For finite spacing a, the Lagrangian can contain any operators that are local, invariant under transverse lattice gauge symmetries and under Poincaré symmetries manifestly preserved by the lattice cutoff, and renormalizable by dimensional counting with respect to the continuum coordinates x^α. The objective is to obtain an approximation to the light-cone Hamiltonian operator P^- that may be diagonalized in a Fock state basis of the above fields. This may be achieved by first fixing to the light-cone gauge $A_-=0$, eliminating non-dynamical fields, then expanding the resulting Hamiltonian in powers of the remaining dynamical fields. Truncation of such a ''color-dielectric'' expansion is a valid approximation provided wave functions of interest (typically those of the lightest eigenstates) are dominated by few-body Fock states. This is achieved by working in a region of coupling space with sufficiently heavy dynamical fields. This in turn will be found to constrain the transverse lattice spacing a to be coarse when symmetries and phenomenology are optimized.

The Lagrangian density we consider contains terms up to orders M^4 and $\bar{\Psi}M\Psi$ for the large-N_c theory

$$
\begin{aligned}
L=\sum_{\mathbf{x}}\int dx^- \sum_{\alpha,\beta=+,-}\sum_{r=1,2} & -\frac{1}{2G^2}\mathrm{Tr}\{F^{\alpha\beta}(\mathbf{x})F_{\alpha\beta}(\mathbf{x})\} \\
& +\mathrm{Tr}\{\bar{D}_\alpha M_r(\mathbf{x})(\bar{D}^\alpha M_r(\mathbf{x}))^\dagger\}-\mu_b^2\mathrm{Tr}\{M_rM_r^\dagger\} \\
& +i\bar{\Psi}\gamma^\alpha(\partial_\alpha+iA_\alpha)\Psi-\mu_f\bar{\Psi}\Psi \\
& +i\kappa_a[\bar{\Psi}(\mathbf{x})\gamma^r M_r(\mathbf{x})\Psi(\mathbf{x}+a\hat{\mathbf{r}}) \\
& -\bar{\Psi}(\mathbf{x})\gamma^r M_r^\dagger(\mathbf{x}-a\hat{\mathbf{r}})\Psi(\mathbf{x}-a\hat{\mathbf{r}})] \\
& +\kappa_s[\bar{\Psi}(\mathbf{x})M_r(\mathbf{x})\Psi(\mathbf{x}+a\hat{\mathbf{r}}) \\
& +\bar{\Psi}(\mathbf{x})M_r^\dagger(\mathbf{x}-a\hat{\mathbf{r}})\Psi(\mathbf{x}-a\hat{\mathbf{r}})]-V_{\mathbf{x}},
\end{aligned}
\tag{3}
$$

where $F^{\alpha\beta}(\mathbf{x})$ is the continuum field strength in the (x^0,x^3) planes at each $\mathbf{x}$,

$$
\bar{D}_\alpha M_r(\mathbf{x})=[\partial_\alpha+iA_\alpha(\mathbf{x})]M_r(\mathbf{x})-iM_r(\mathbf{x})A_\alpha(\mathbf{x}+a\hat{\mathbf{r}}),
\tag{4}
$$

and the link-field potential is

$$
\begin{aligned}
V_{\mathbf{x}}=& -\frac{\beta}{N_c a^2}\sum_{r\neq s}\mathrm{Tr}\{M_r(\mathbf{x})M_s(\mathbf{x}+a\hat{\mathbf{r}})M_r^\dagger(\mathbf{x}+a\hat{\mathbf{s}})M_s^\dagger(\mathbf{x})\} \\
& +\frac{\lambda_1}{a^2N_c}\sum_r\mathrm{Tr}\{M_rM_r^\dagger M_rM_r^\dagger\} \\
& +\frac{\lambda_2}{a^2N_c}\sum_r\mathrm{Tr}\{M_r(\mathbf{x})M_r(\mathbf{x}+a\hat{\mathbf{r}})M_r^\dagger(\mathbf{x}+a\hat{\mathbf{r}})M_r^\dagger(\mathbf{x})\} \\
& +\frac{\lambda_4}{a^2N_c}\sum_{\sigma=\pm2,\sigma'=\pm1}\mathrm{Tr}\{M_\sigma^\dagger M_\sigma M_{\sigma'}^\dagger M_{\sigma'}\}.
\end{aligned}
\tag{5}
$$

We have defined $M_r=M_{-r}^\dagger$ and hold $\bar{G}\to G\sqrt{N_c}$ finite as $N_c\to\infty$. To this action we could in principle add allowed operators at order is M^6, $(\bar{\Psi}\Psi)^2$, $\Psi M^2\Psi$, and so on. It should therefore be understood as the truncation of an expansion in powers of the fields. Strictly speaking, this expansion should be performed for the light-cone gauge-fixed Hamiltonian in terms of dynamical fields only.

In the chiral representation, $\Psi^\dagger=(u_+^*,v_+^*,v_-^*,u_-^*)/2^{1/4}$ decomposes into complex fermion fields v (u) with a helicity subscript $h=\pm$ denoting the sign of the eigenvalue of γ^5. In light-cone gauge $A_-=0$, A_+ and $v_\pm$ are non-dynamical (independent of light-cone time x^+) and are eliminated at the classical level using the equations of motion

$$
(\partial_-)^2A_+=\frac{G^2}{2}\left(J^+-\frac{1}{N}\mathrm{Tr}J^+\right),
\tag{6}
$$

$$
i\partial_-v_h=\frac{\mu_f}{\sqrt{2}}F_{-h},
\tag{7}
$$

where we have defined

$$F_h(\mathbf{x}) = -u_h(\mathbf{x}) + \frac{\kappa_s}{\mu_f}\sum_r [M_r(\mathbf{x})u_h(\mathbf{x}+a\hat{\mathbf{r}}) + M_r^\dagger(\mathbf{x} - a\hat{\mathbf{r}})u_h(\mathbf{x}-a\hat{\mathbf{r}})] + \frac{hi\kappa_a}{\mu_f}\{M_1(\mathbf{x})u_{-h}(\mathbf{x}+a\hat{1}) - hiM_2(\mathbf{x})u_{-h}(\mathbf{x}+a\hat{2}) - M_1^\dagger(\mathbf{x}-a\hat{\mathbf{1}})u_{-h}(\mathbf{x}-a\hat{1}) + hiM_2^\dagger(\mathbf{x}-a\hat{\mathbf{2}})u_{-h}(\mathbf{x}-a\hat{\mathbf{2}})\}, \quad (8)$$

$$J^+(\mathbf{x}) = i\sum_r [M_r(\mathbf{x})\overleftrightarrow{\partial}_- M_r^\dagger(\mathbf{x}) + M_r^\dagger(\mathbf{x}-a\hat{\mathbf{r}})\overleftrightarrow{\partial}_- M_r(\mathbf{x} - a\hat{\mathbf{r}})] + \sum_h u_h(\mathbf{x})u_h^\dagger(\mathbf{x}). \quad (9)$$

The lightcone Hamiltonian, expressed in terms of the remaining dynamical fields $u_\pm(\mathbf{x})$ and $M_r(\mathbf{x})$, may be obtained from the action (3) in the standard way [3]

$$P^- = \int dx^- \sum_{\mathbf{x}} \frac{G^2}{4}\left(\mathrm{Tr}\left\{J^+\frac{1}{(i\partial_-)^2}J^+\right\} - \frac{1}{N_c}\mathrm{Tr}\{J^+\}\frac{1}{(i\partial_-)^2}\mathrm{Tr}\{J^+\}\right) + \frac{\mu_f^2}{2}\sum_h\left(F_h^\dagger\frac{1}{i\partial_-}F_h\right) + V_{\mathbf{x}}[M]. \quad (10)$$

Under certain reasonable assumptions [8], the Hamiltonian (10) is a truncation of the most general Hamiltonian to orders M^4 and uMu. It also contains some, but not all, allowed operators at orders uM^2u and u^4. In particular, it contains the combination $J^+\partial_-^{-2}J^+$, which is responsible for confinement in the lattice theory of states singlet under residual x^--independent gauge transformation [2]. The various parameters $G, \mu_f, \kappa_a, \kappa_s, \mu_b, \lambda_1, \lambda_2, \lambda_4, \beta$, as well as ones that would appear at higher orders of the color-dielectric expansion, are coupling constants that will run with the cutoff(s) in the theory. In principle, this running could be determined by performing renormalization group transformations from QCD at short distance scales. However, on a coarse lattice, weak-coupling perturbation theory is not available, and such an approach become unworkable. One may also treat the problem as an effective field theory, fixing couplings phenomenologically. Even in this case, one may constrain the parameters from first principles by empirically tuning them to minimize the violation of continuum symmetries. In the case of pure gauge theories, at lowest order of the color-dielectric expansion, this gave a quite accurate estimate of the running couplings, without the need to resort to "phenomenology" [5]. For meson calculations with our choice of Hamiltonian (10), additional phenomenological constraints must be used to obtain unambiguous values for the coupling constants, although symmetry requirements do strongly constrain them.

Of the other generators of the Poincaré algebra, $P^\nu, M^{\mu\nu}$, the following can be derived canonically at $x^+=0$:

$$P^+ = \int dx^- \sum_{\mathbf{x},s,h} 2\mathrm{Tr}\{\partial_- M_s(\mathbf{x})\partial_- M_s(\mathbf{x})^\dagger\} + iu_h^*\partial_- u_h, \quad (11)$$

$$M^{-+} = \int dx^- \sum_{\mathbf{x},s,h} x^-\left\{2\mathrm{Tr}\{\partial_- M_s(\mathbf{x})\partial_- M_s(\mathbf{x})^\dagger\} + \frac{i}{2}u_h^*\overleftrightarrow{\partial}_- u_h\right\}, \quad (12)$$

$$M^{+r} = -\int dx^- \sum_{\mathbf{x},s,h} 2\left(x^r + \frac{a}{2}\delta^{rs}\right)\mathrm{Tr}\{\partial_- M_s(\mathbf{x})\partial_- M_s(\mathbf{x})^\dagger\} + ix^r u_h^*\partial_- u_h. \quad (13)$$

Note that these are all kinematic operators, quadratic in fields. P^+ and M^{-+} generate translations and boosts respectively in the x^- direction and are unaffected by the transverse lattice cutoff. The cutoff effects on the boost-rotation operator M^{+r} are discussed further in the next section.

B. Space of states

For the construction of a Fock space of the dynamical fields M_r and u_h, it is convenient to Fourier transform the fields in the x^- coordinate only. Thus, we introduce a Fock space operator $a_{r,ij}^\dagger(k^+,\mathbf{x})$ which creates a "link parton" with light-cone momentum k^+, carrying color $i \in \{1,\ldots,N_c\}$ at site $\mathbf{x}$ to color j at site $\mathbf{x}+a\hat{\mathbf{r}}$; $a_{-r,ij}^\dagger$ creates an oppositely oriented link parton. Likewise, $b_{h,i}^*(k^+,\mathbf{x})$ creates a "quark parton" of helicity h, color i, momentum k^+ at site $\mathbf{x}$, while d^* does the same for anti-quarks. We have

$$[a_{\lambda,ij}(k^+,\mathbf{x}), a_{\rho,kl}^*(\tilde{k}^+,\mathbf{y}] = \delta_{ik}\delta_{jl}\delta_{\lambda\rho}\delta_{xy}\delta(k^+-\tilde{k}^+), \quad (14)$$

$$[a_{\lambda,ij}(k^+,\mathbf{x}), a_{\rho,kl}(\tilde{k}^+,\mathbf{y})] = 0, \quad (15)$$

$$\{b_{h,i}(k^+,\mathbf{x}), b_{h',j}^*(\tilde{k}^+,\mathbf{y})\} = \delta_{ij}\delta_{hh'}\delta_{\mathbf{xy}}\delta(k^+-\tilde{k}^+), \quad (16)$$

$$\{b_{h,i}(k^+,\mathbf{x}), b_{h',j}(\tilde{k}^+,\mathbf{y})\} = 0, \quad (17)$$

where λ and $\rho \in \{\pm 1, \pm 2\}$ denote the orientations of link variables in the (x^1,x^2) plane, $a_{\lambda,ij}^* = a_{\lambda,ji}^\dagger$, and similar anti-commutators exist for d. Fock space is already diagonal in the light-cone momentum P^+ and serves as a basis for finding the eigenfunctions P^-, the light-cone wave functions. As usual in light-cone quantization (without zero modes), the Fock vacuum state $|0\rangle$ is an exact eigenstate of P^-.

Further cutoffs, apart from the transverse lattice, must be applied to Fock space to make it finite dimensional. We will use discrete light cone quantization (DLCQ) [10,11] to discretize light-cone momentum, which amounts to compactifying x^- on circle of circumference $\mathcal{L} = 2\pi K/P^+$, where K is a positive integer, with periodic (anti-periodic) boundary conditions for $M(u)$. Eventually, we will extrapolate observ-

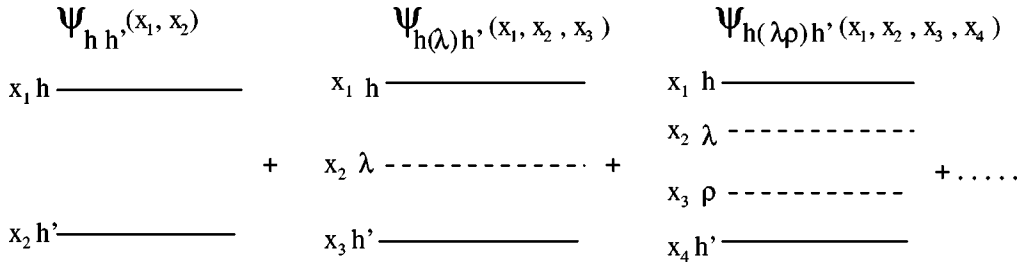

FIG. 1. Planar diagram representation of the Fock space structure of a meson boundstate. Solid lines represent quarks/anti-quarks, chain lines link fields.

ables to $K=\infty$. The use of anti-periodic boundary conditions is desirable because it tends to improve convergence as $K\to\infty$. However, one cannot consistently have anti-periodic boundary conditions for both bosons and fermions in a theory with Yukawa-type interactions.

To reduce the size of Fock space still further, it will be convenient to impose a separate Tamm-Dancoff cutoff on the maximum number of partons in Fock space, studying the theory as this cutoff is raised. Since the large N_c limit automatically restricts to a quark–anti-quark pair in the meson sector, this effectively means a cut off on the number of link partons. A general meson state of light-cone momentum P^+, which is translationally invariant in the transverse direction, takes the form

$$
\begin{aligned}
|\psi(P^+)\rangle=&\frac{2a\sqrt{\pi}}{\sqrt{N_c}}\sum_{\mathbf{x}}\sum_{h,h'}\int_0^{P^+}dk_1^+dk_2^+\,\delta(P^+-k_1^+-k_2^+)\{\psi_{hh'}(x_1,x_2)b_h^\dagger(k_1^+,\mathbf{x})d_{h'}^\dagger(k_2^+,\mathbf{x})|0\rangle\}\\
&+\frac{2a\sqrt{\pi}}{N_c}\sum_{\mathbf{x}}\sum_{h,h',r}\int_0^{P^+}\frac{dk_1^+dk_2^+dk_3^+}{P^+}\,\delta(P^+-k_1^+-k_2^+-k_3^+)\{\psi_{h(r)h'}(x_1,x_2,x_3)b_h^\dagger(k_1^+,\mathbf{x})a_r^\dagger(k_2^+,\mathbf{x})d_{h'}^*\\
&\times(k_3^+,\mathbf{x}+a\hat{\mathbf{r}})|0\rangle+\psi_{h(-r)h'}(x_1,x_2,x_3)b_h^\dagger(k_1^+,\mathbf{x}+a\hat{\mathbf{r}})a_{-r}^\dagger(k_2^+,\mathbf{x})d_{h'}^*(k_3^+,\mathbf{x})|0\rangle\}\\
&+\frac{2a\sqrt{\pi}}{\sqrt{N_c^3}}\sum_{\mathbf{x}}\sum_{h,h',r,s}\int_0^{P^+}\frac{dk_1^+dk_2^+dk_3^+dk_4^+}{(P^+)^2}\,\delta(P^+-k_1^+-k_2^+-k_3^+-k_3^+)\\
&\times\{\psi_{h(rs)h'}(x_1,x_2,x_3,x_4)b_h^\dagger(k_1^+,\mathbf{x})a_r^\dagger(k_2^+,\mathbf{x})a_s^\dagger(k_3^+,\mathbf{x}+a\hat{\mathbf{r}})d_{h'}^*(k_4^+,\mathbf{x}+a\hat{\mathbf{r}}+a\hat{\mathbf{s}})|0\rangle\\
&+\psi_{h(r-s)h'}(x_1,x_2,x_3,x_4)b_h^\dagger(k_1^+,\mathbf{x})a_r^\dagger(k_2^+,\mathbf{x})a_{-s}^\dagger(k_3^+,\mathbf{x}+a\hat{\mathbf{r}}-a\hat{\mathbf{s}})d_{h'}^*(k_4^+,\mathbf{x}+a\hat{\mathbf{r}}-a\hat{\mathbf{s}})|0\rangle\\
&+\psi_{h(-rs)h'}(x_1,x_2,x_3,x_4)b_h^\dagger(k_1^+,\mathbf{x}+a\hat{\mathbf{r}})a_{-r}^\dagger(k_2^+,\mathbf{x})a_s^\dagger(k_3^+,\mathbf{x})d_{h'}^*(k_4^+,\mathbf{x}+a\hat{\mathbf{s}})|0\rangle\\
&+\psi_{h(-r-s)h'}(x_1,x_2,x_3,x_4)b_h^\dagger(k_1^+,\mathbf{x}+a\hat{\mathbf{r}})a_{-r}^\dagger(k_2^+,\mathbf{x})a_{-s}^\dagger(k_3^+,\mathbf{x}-a\hat{\mathbf{s}})d_{h'}^*(k_4^+,\mathbf{x}-a\hat{\mathbf{s}})|0\rangle\}+\cdots,
\end{aligned}
\tag{18}
$$

where states with up to two links have been explicitly displayed. In Eq. (18), † acts on gauge indices and $x_1=k_1^+/P^+$, etc., are light-cone momentum fractions. Only gauge singlet combinations under residual gauge transformations in $A_-=0$ gauge can contribute to states of finite energy [2]. Because pair production of quarks and mixing with glueballs is suppressed at large N_c, the states (18) provide a description of the valence quark content of flavor non-singlet mesons. Thus, one should implicitly understand a distinct flavor label on the quark and anti-quark, which is redundant. The sequence of orientations $\lambda,\rho,\ldots$ of link variables and the P^+ momentum fractions $x_1,x_2,\ldots$ are sufficient to encode the internal transverse and longitudinal structure respectively of Fock states contributing to the bound state. Thus, including quark helicities h,h', a general Fock state may be labeled

$$
|(x_1,h),(x_2,\lambda),\ldots,(x_{n-1},\rho),(x_n,h')\rangle. \tag{19}
$$

The expansion (18) may be represented by a planar (large-N_c) diagram notation shown in Fig. 1. This will be helpful when enumerating the matrix elements of the Hamiltonian.

The transverse momentum operator is not directly defined because of the lattice regulator, but one may introduce transverse momentum $\mathbf{P}$ by application of the boost-rotation operator M^{+r}. Let $|(x_1,\mathbf{x}_1),\ldots,(x_n,\mathbf{x}_n)\rangle$ denote an n-parton Fock state. $\mathbf{x}_p$ is the transverse position and x_p the P^+ mo-

mentum fraction of the pth parton (conventionally we take transverse position to be the midpoint of a link, for link fields). Using (13) we find

$$\exp[-iM^{+r}P_r/P^+]|(x_1,\mathbf{x}_1),\ldots,(x_n,\mathbf{x}_n)\rangle = \exp\left[i\mathbf{P}\cdot\sum_{p=1}^{n}x_p\mathbf{x}_p\right]|(x_1,\mathbf{x}_1),\ldots,(x_n,\mathbf{x}_n)\rangle. \quad (20)$$

Therefore, the net effect is to add phase factors into matrix elements of P^- between Fock states at $\mathbf{P}=0$. In a Poincaré covariant or a free theory, the transformation (20) applied to eigenstates of P^- (18) would be sufficient to generate eigenstates of P^- at non-zero $\mathbf{P}$. However, the lattice regulator spoils Poincaré covariance and in general one must rediagonalize P^- after boosting Fock states by Eq. (20). Thus, the eigenfunctions ψ in Eq. (18) for P^- will become functions of $\mathbf{P}$ also.

The state is normalized covariantly

$$\langle\psi(P_1^+,\mathbf{P}_1)|\psi(P_2^+,\mathbf{P}_2)\rangle = 2P_1^+(2\pi)^3\delta(P_1^+-P_2^+)\,\delta(\mathbf{P}_1-\mathbf{P}_2), \quad (21)$$

if

$$1=\int_0^1 dx\sum_{h,h'}|\psi_{hh'}(x,1-x)|^2 + \int_0^1 dx_1dx_2\sum_{h,\lambda,h'}|\psi_{h(\lambda)h'}(x_1,x_2,1-x_1-x_2)|^2 + \int_0^1 dx_1dx_2dx_3\sum_{h,\lambda,\rho,h'} \times|\psi_{h(\lambda\rho)h'}(x_1,x_2,x_3,1-x_1-x_2-x_3)|^2+\cdots \quad (22)$$

for any $\mathbf{P}_1,\mathbf{P}_2$. This also ensures that the light-cone momentum sum rule is satisfied, even at finite DLCQ cutoff K, since translation invariance in the x^- direction is preserved by DLCQ.

Since there is 90° rotational symmetry about x^3 for a state with $\mathbf{P}=0$, it is possible to distinguish the angular momentum projections $\mathcal{J}_3$ mod 4. There is also exact symmetry under $\mathcal{G}$ parity, charge conjugation $\mathcal{C}$, and transverse reflections in the x^1 and x^2 directions, $\mathcal{P}_1,\mathcal{P}_2$. Although the parity $\mathcal{P}=\mathcal{P}_1\mathcal{P}_2\mathcal{P}_3$ is dynamical and in general broken, one can associate a parity to bound states from their behavior under the free particle limit of $\mathcal{P}_3$. Indeed, there is a Z_2 kinematic symmetry

$$\mathcal{P}_f\psi_{hh'}(1-x,x)\to\psi_{hh'}(x,1-x), \quad (23)$$

which corresponds to the free $\mathcal{P}_3$ operation in the zero-link sector that is exact at any cut-off K. In this way, one has enough information to identify the $\mathcal{J}^{\mathcal{PC}}$ structure of light states unambiguously.

In general, we will find that the lightest mesons are 0^{-+} and 1^{--}, with the former lying lower in mass. It is thus natural to compare them with the physical pion and rho. Because of violations of covariance, the $\mathcal{J}_3=0$ component of the 1^{--} (ρ_0) will also split from its $\mathcal{J}_3=\pm1$ components ($\rho_\pm$) which are always degenerate on the transverse lattice at $\mathbf{P}=0$. In view of the low-energy nature of the truncation of the color-dielectric expansion, we do not analyze heavier mesons, although their eigenfunctions are obtained as a by product of our calculations.

C. Renormalization

We have constructed a gauge theory with transverse lattice and Tamm-Dancoff cutoffs that we do not intend to extrapolate and a DLCQ cutoff that we do. The first step in the renormalization process is to ensure finiteness of physical observables in the limit $K\to\infty$. It turns out that divergences exist but they require only infinite and finite self-energy counterterms that renormalize existing parton mass terms in the light-cone Hamiltonian. The remaining cutoffs that are not extrapolated obviously violate Lorentz covariance. This violation can however be minimized by appropriate finite renormalization of all the couplings appearing in P^- (10). In this section we describe our procedure for performing these finite and infinite renormalizations.

It is convenient to use one of the parameters of the Hamiltonian to set the dimensionful scale of the theory and define dimensionless versions of the others. Conventionally we will use $\overline{G}$ to set the scale, which has the dimensions of mass. It will later be related to the QCD mass scale by calculation of the heavy source potential [6]. The following dimensionless parameters are then introduced:

$$\frac{\mu_b}{\overline{G}}\to m_b;\quad \frac{\mu_f}{\overline{G}}\to m_f;\quad \kappa_a\sqrt{\frac{N_c}{G}}\to k_a;\quad \kappa_s\sqrt{\frac{N_c}{G}}\to k_s;$$
$$\frac{\lambda_i}{\overline{G}^2}\to l_i\ (i=1,2,4);\quad \frac{\beta}{\overline{G}^2}\to b. \quad (24)$$

Since we will need to study the meson eigenfunctions of P^- as a function of P^+ and $\mathbf{P}$, let us write, for these eigenfunctions,

$$2P^+P^-=\mathcal{M}^2+R(\mathbf{P}), \quad (25)$$

such that $R(0)=0$. $\mathcal{M}^2$ is the invariant mass (squared). We begin with $\mathbf{P}=0$, in which case the non-zero Fock space matrix elements of the dimensionless invariant mass operator

$$\langle(y_1,h_1),(y_2,\sigma),\ldots,(y_{n-1},\tau),(y_n,h_2)|2P^+P^-/\overline{G}^2| \times(x_1,h_1'),(x_2,\lambda),\ldots,(x_{n-1},\rho),(x_n,h_2')\rangle \quad (26)$$

are enumerated in Figs. 2(a)–(m) and Table I. A number of comments are necessary to explain these amplitudes. We have defined

$$\mathrm{Rot}[\lambda,\rho]\equiv\epsilon_{|\lambda||\rho|}\mathrm{Sgn}[\lambda]\mathrm{Sgn}[\rho]. \quad (27)$$

In the planar diagram vertices of Fig. 2, light-cone momentum fraction (x,y,z), quark helicity (h,h'), and link-field orientation $(\lambda,\rho,\sigma,\tau)$ labels are given where necessary.

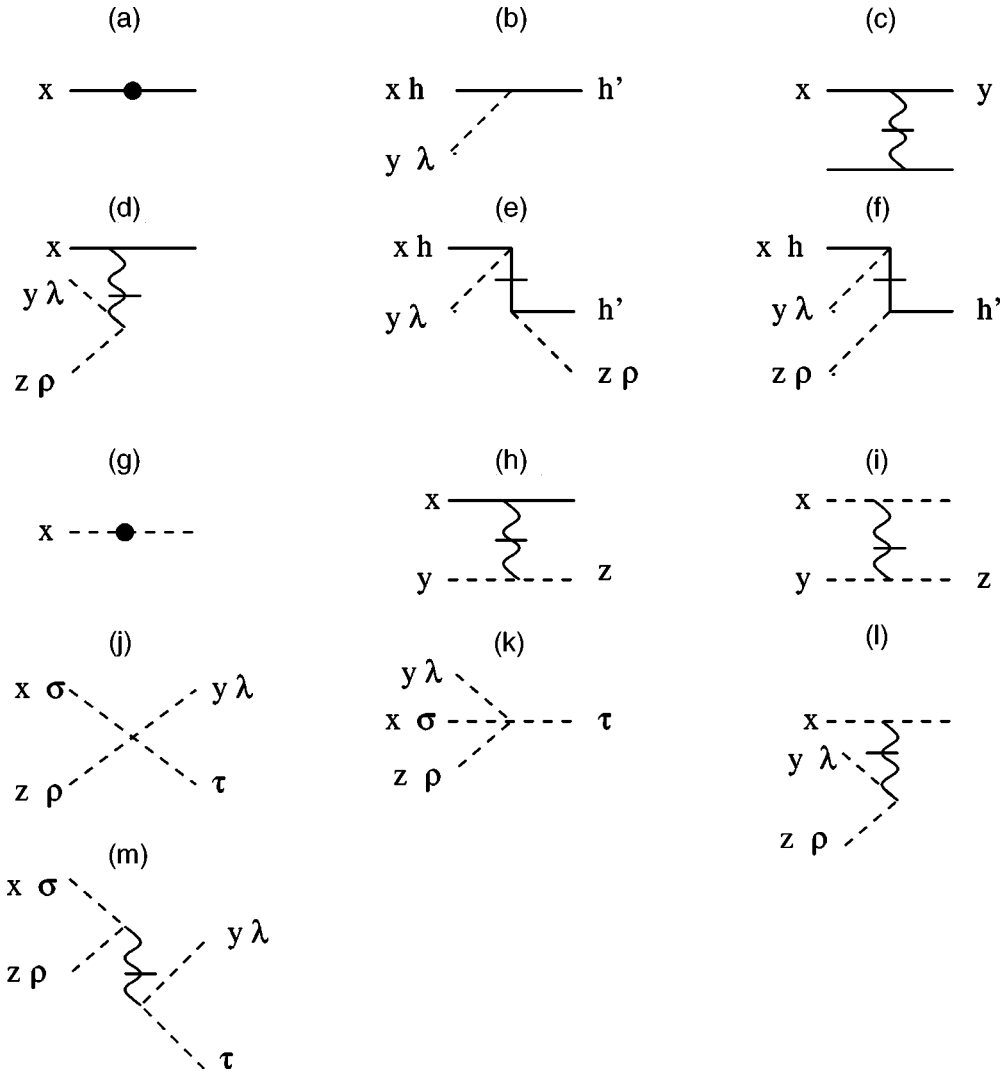

FIG. 2. Planar diagram representation of the elementary amplitudes contributing to Eq. (26). Vertical barred lines are x^+-instantaneous interactions.

Lines with a bar denote the x^+-instantaneous propagators ∂_-^{-1} and ∂_-^{-2} for v quarks and A_+ gauge fields respectively. ''P'' denotes that a principal value prescription is used when integrating light-cone continuum momentum fraction across singularities. For simplicity, we have not shown vertices involving only anti-quarks, which are similar to those involving only quarks. To these diagrams we add planar spectator lines which go to make up the full gauge singlet Fock state.

At finite transverse lattice spacing a, but before the light-cone DLCQ cutoff K is imposed, the theory is behaving like a continuum $(1+1)$-dimensional gauge theory coupled to a set of fundamental fermion and adjoint scalar fields [12]. Although super-renormalizable in the $(1+1)$-dimensional sense, the light-cone quantization in light-cone gauge introduces its own characterstic divergences due to the presence of non-local instantaneous interations. Those originating from the instantaneous gluon propagator $1/\partial_-^2$ are dealt with by the principal value prescription in the manner established by 't Hooft [13]. Those originating from the instantaneous quark propagator $1/\partial_-$ have been studied by Burkardt [14], whose analysis we briefly recall.

A basic one-loop logarithmic divergence occurs in the quark self-energy as represented in the light-cone perturbation theory diagram of Fig. 3(a) as the quark loop momentum vanishes. The cubic vertices are of the same type, with coupling either $m_f k_a$ or $m_f k_s$, once the orientations of the intermediate link fields have been summed over. The divergences are cancelled, in these diagrams and any others obtained by adding spectators, by an infinite quark ''kinetic'' mass counterterm in the Hamiltonian [Fig. 3(b)]

$$\frac{(k_a^2+k_s^2)}{\pi}\int_0^x \frac{dy}{y}. \tag{28}$$

This is not sufficient for the divergences in the two-loop diagrams of Figs. 4(a)–(c) to cancel. One may add a finite kinetic mass counterterm δm^2, adjusted at order (k_a^2,k_s^2), to produce finite results when Fig. 4(d) is included. Higher-loop generalizations of the same diagrams are also rendered finite by adjusting δm^2 at higher orders in k_a and k_s. Dressing loop diagrams with instantaneous gluon lines (e.g. Fig. 5) renders them individually finite. As in Ref. [14], our own

TABLE I. Matrix elements of the dimensionless invariant mass operator $2P^+P^-/\overline{G}^2$ in Fock space. Momentum conserving delta functions are omitted for clarity.

$\frac{1}{x}\left(m_f^2+\delta m_p^2+\frac{(k_a^2+k_s^2)}{\pi}\int_0^x\frac{dy}{y}\right)$	(a)
$\frac{1}{2\sqrt{\pi y}}\left(\frac{1}{x+y}-\frac{1}{x}\right)\{m_f k_s+m_f k_a \mathrm{Sgn}[\lambda](\delta_{\lvert\lambda\rvert 2}-ih\delta_{\lvert\lambda\rvert 1})\}$	(b)
$\frac{-1}{2\pi}P\left(\frac{1}{(x-y)^2}\right)$	(c)
$\frac{-(y-z)}{4\pi(y+z)^2\sqrt{yz}}\delta_{-\lambda\rho}$	(d)
$\frac{1}{4\pi(x+y)\sqrt{yz}}\{k_s^2\delta_{hh'}+k_a^2\delta_{hh'}(\delta_{\lambda\rho}-\delta_{-\lambda\rho}-ih\mathrm{Rot}[\lambda,\rho])$ $+k_a k_s\delta_{-hh'}[\mathrm{Sgn}[\lambda](ih\delta_{\lvert\lambda\rvert 1}-\delta_{\lvert\lambda\rvert 2})+\mathrm{Sgn}[\rho](ih\delta_{\lvert\rho\rvert 1}-\delta_{\lvert\rho\rvert 2})]\}$	(e)
$\frac{1}{4\pi(x+y)\sqrt{yz}}\{k_s^2\delta_{hh'}+k_a^2\delta_{hh'}(\delta_{-\lambda\rho}-\delta_{\lambda\rho}+ih\mathrm{Rot}[\lambda,\rho])$ $+k_a k_s\delta_{-hh'}(\mathrm{Sgn}[\lambda](ih\delta_{\lvert\lambda\rvert 1}-\delta_{\lvert\lambda\rvert 2})-\mathrm{Sgn}[\rho](ih\delta_{\lvert\rho\rvert 1}-\delta_{\lvert\rho\rvert 2}))\}$	(f)
$\frac{m_b^2}{x}$	(g)
$\frac{-1}{4\pi}P\left(\frac{y+z}{\sqrt{zy}(z-y)^2}\right)$	(h)
$\frac{-1}{8\pi}P\left(\frac{(y+z)(2x+y-z)}{\sqrt{xzy(x+y-z)}(z-y)^2}\right)$	(i)
$\frac{1}{4\pi\sqrt{xyz(x+z-y)}}\{2l_1\delta_{\sigma\lambda}\delta_{\rho\tau}\delta_{-\rho\sigma}+l_2(\delta_{\sigma\lambda}\delta_{\rho\tau}\delta_{\rho\sigma}+\delta_{-\sigma\rho}\delta_{-\lambda\tau}\delta_{-\sigma\lambda})$ $+l_4(\delta_{\sigma\lambda}\delta_{\rho\tau}\lvert\mathrm{Rot}[\sigma,\rho]\rvert+\delta_{-\sigma\rho}\delta_{-\lambda\tau}\lvert\mathrm{Rot}[\sigma,\lambda]\rvert)-b\delta_{\lambda\rho}\delta_{\sigma\tau}\lvert\mathrm{Rot}[\sigma,\rho]\rvert\}$	(j)
$\frac{1}{4\pi\sqrt{xyz(x+z+y)}}\{2l_1\delta_{-\sigma\lambda}\delta_{\lambda\tau}\delta_{\lambda\rho}+l_2\delta_{\sigma\tau}\delta_{-\lambda\rho}\delta_{\lvert\lambda\rvert\lvert\sigma\rvert}$ $+l_4(\delta_{-\lambda\sigma}\delta_{\rho\tau}\lvert\mathrm{Rot}[\lambda,\rho]\rvert+\delta_{-\sigma\rho}\delta_{\lambda\tau}\lvert\mathrm{Rot}[\sigma,\lambda]\rvert)-b\delta_{-\lambda\rho}\delta_{\sigma\tau}\lvert\mathrm{Rot}[\sigma,\lambda]\rvert\}$	(k)
$\frac{-1}{8\pi}\frac{(y-z)(2x+y+z)}{\sqrt{xzy(x+y+z)}(z+y)^2}\delta_{-\lambda\rho}$	(l)
$\frac{-1}{8\pi}\frac{(x-z)(2y-x-z)}{\sqrt{xzy(x-y+z)}(z+x)^2}\delta_{-\sigma\rho}\delta_{-\lambda\tau}$	(m)

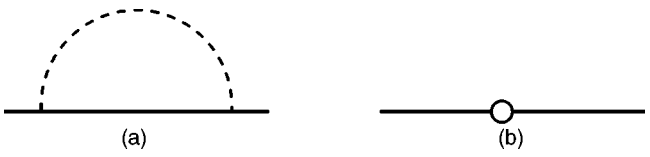

FIG. 3. (a) one-loop logarithmically divergent quark self-energy, (b) logarithmically divergent mass insertion counterterm represented by open circle.

checks of these statements for the transverse lattice theory have been done only in perturbation theory, but we will assume they are true to all orders. It was also shown in Ref. [14], by means of simple cases, that choosing the correct counterterm δm^2 was equivalent to restoring parity invariance, which is not manifest in light-cone coordinates.

By adjusting the finite counterterm δm^2, one ensures that the $K\to\infty$ limit can be taken when DLCQ is used. However, it was pointed out by Burkardt that, while this ensures a

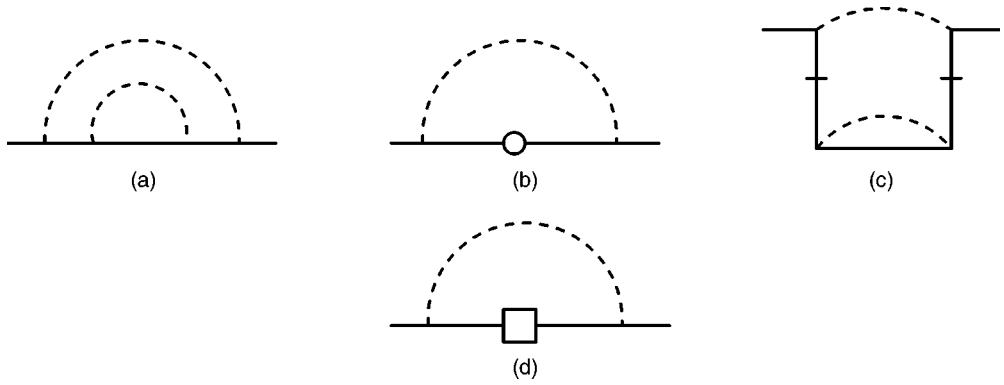

FIG. 4. (a),(c) two-loop logarithmically divergent quark self-energies, (b) one-loop diagram with infinite mass insertion, (d) one-loop diagram with finite mass insertion δm^2 represented by open box.

finite answer for the $K\to\infty$ limit of the self-energy, the use of a momentum-independent mass counterterm in DLCQ will not yield the same as the covariant answer for the same couplings. In effect DLCQ produces a finite violation of covariance. This is one of a number of sources covariance violation in our calculation. Rather than analyzing how one might minimize the individual violations—it is not obvious which are the most significant—we will perform overall covariance tests on the bound state wave functions that are the end product.

A Tamm-Dancoff cutoff on the maximum number of link fields in a state also violates covariance. In principle, this can be compensated by introducing spectator-dependent counterterms [15]. In practice that will lead to too many couplings for viable calculation at a physically reasonable choice of Tamm-Dancoff cutoff. However, it is necessary for finiteness of the quark self-energy to use spectator-dependent finite counterterms δm^2. Therefore, we must introduce separate counterterms δm_p^2 for the Fock sector containing p links (note that the sector with p maximum has no finite or infinite quark self-energy counterterms). These are adjusted to produce finite quark self-energy in addition to optimization of covariance of hadron wave functions. Since we work at the level of hadrons, the quark self-energy is tested indirectly. A tachyonic quark self-energy, whether divergent or not, would be signalled by tachyonic behavior in the lightest hadron mass. Therefore, we test for absence of such a divergence in the ligthest mass as $K\to\infty$. A positive divergent quark self-energy would artificially suppress the lowest Fock sectors, that are subject to loop corrections and counterterms, in the hadron wave function as $K\to\infty$ (the hadron mass may remain finite). Therefore, we test for absence of this suppression, in particular, by fitting f_π which is a measure of the $p=0$ Fock component.

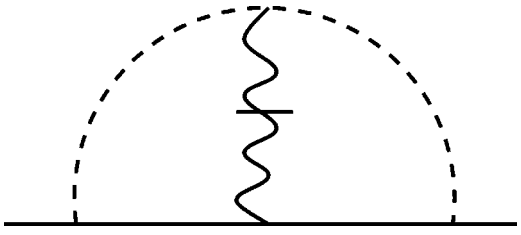

FIG. 5. Finite diagram with instantaneous interaction dressing.

In summary, taking the $K\to\infty$ limit with a Tamm-Dancoff cutoff on link fields in place, one must introduce infinite and spectator-dependent finite self-energy counterterms. Even though the theory is now finite, Poincaré covariance is still violated by the finite transverse lattice spacing a, the Tamm-Dancoff cutoff, and by the use of momentum-independent finite-mass counterterms δm_p^2. We propose to minimize these violations by finitely renormalizing all the couplings available in P^-.

For perfectly relativistic dispersion, $R(\mathbf{P})=|\mathbf{P}|^2$ for every eigenfunction in Eq. (25); this will receive corrections on the coarse transverse lattice. To quantify the covariance violation we will expand the dispersion relation for each bound state

$$R(\mathbf{P})=c^2|\mathbf{P}|^2+O(\mathbf{P}^4). \tag{29}$$

The transverse speed of light c will in general differ from one (the speed in the x^3 direction). A simple criterion, which worked well in previous studies, is to minimize this difference in the low lying eigenstates of P^-, ignoring the anharmonic terms in R.

The same procedure may be carried out for glueball bound states to constrain the pure-glue interactions in the Hamiltonian, independently of the meson sector (at large N_c). In addition, the rotational invariance of the potential between heavy sources may be optimized. These latter tests have been described in detail in previous work [5]. We will use the string tension $\sqrt{\sigma}$ from the potential to set the QCD scale from experiment.

The transverse lattice Lagrangian (3) contains terms that also violate chiral symmetry explicitly, via the couplings m_f and k_s. Since we work at the level of hadrons, a measure of chiral current non-conservation is provided by the pion mass in a covariant stable theory, as a result of the PCAC (partial conservation of axial vector current) theorem. This measure loses accuracy if the theory also has significant explicit covariance violation, as in our case. The explicit violation of chiral symmetry could be minimized by tuning further chiral-symmetry violating counterterms, which we discuss in the Appendix. However, these lie at higher order of the color-

TABLE II. Optimum coupling constants at $a=2/3$ fm for a three-link truncation. Note that δm_0^2 was swept more coarsely than the other couplings.

m_b	b	l_1	l_2	l_4	k_s	k_a	m_f	δm_0^2	δm_1^2	δm_2^2
0.276	0.768	−0.169	−0.186	0.024	0.420	0.652	0.236	1	−0.127	−0.035

dielectric expansion. In the present calculation, we finitely renormalize the Hamiltonian to fit the experimental pion mass, since this is naively a measure of chiral current conservation. Since the explicit violation of chiral symmetry is actually larger than that suggested by $\mathcal{M}_\pi$, we find that we must also fit the experimental rho mass in order to maintain a realistic pi-rho splitting.

Thus, in addition to optimizing covariance via bound state dispersion, we are proposing to fit four experimental numbers $\mathcal{M}_\pi$, $\mathcal{M}_\rho$, f_π, and $\sqrt{\sigma}$ in order to accurately determine the couplings in our effective Hamiltonian P^-. Since QCD with degenerate flavors contains only two fundamental parameters, the transverse lattice Hamiltonian is not determined from first principles. However, as described above, direct tests of parity and chiral symmetry might allow one to reduce the number of phenomenological parameters further. We leave this for future work.

III. DETERMINATION OF HAMILTONIAN PARAMETERS

In order to reduce the number of coupling variables in the minimization process, this is done in two stages. First, we examine glueball eigenfunctions of P^-, that contain only link fields, and the rotational invariance of the ground state potential between two heavy sources of color. Here we follow, with one exception, exactly the same procedure used in Ref. [5] and so omit all details. The exception is that, instead of using anti-periodic boundary conditions for link fields in x^-, we re-did the calculations with periodic boundary conditions in order to be consistent with the conditions used in the meson sector later. Note that these ''pure-glue'' calculations extrapolate both K and the Tamm-Dancoff cutoff, constraining very precisely the couplings in P^- relevant to that sector (l_1, l_2, l_3, b, m_b) when covariance is optimized. It is not necessary at this stage to use any phenomenological input.

We searched for a trajectory in coupling space that optimized the Poincaré covariance of glueball wave functions and the potential between heavy sources of color. A fairly well-defined one-parameter trajectory is picked out. We choose the best point on that trajectory, which in effect fixes a, corresponding to a value of the link field mass $m_b=0.276$. At this point, we find $\overline{G}\approx 2.75\sqrt{\sigma}$ and $a\overline{G}\approx 4$, where σ is the string tension of the asymptotically linear potential found between two heavy sources. If one takes $\sqrt{\sigma}=440$ MeV, then $\overline{G}\approx 1200$ MeV and $a\approx 2/3$ fm. The values of the other couplings determined by this point are shown in Table II.

Having fixed a subset of the couplings, we fix the remaining ones sensitive only to the meson sector. We investigated the Tamm-Dancoff cutoff up to four links, but show results for a three-link cutoff, since a better sampling of couplings is achievable in this case. The transverse speed of light c is optimized in the dispersion of the 0^{-+} and each component of the 1^{--}, together with the difference between the calculated mass $\mathcal{M}_\pi$ of the 0^{-+} state and the physical pion value. As described in the previous section, we find we must include fits to the physical values of $\mathcal{M}_\rho$ and f_π in the optimization procedure in order to accurately pin down the remaining undetermined couplings of the Hamiltonian, which are shown in Table II.

Table III shows information on the states we identify with the pion and rho at these couplings. One notes that the spin ± 1 projections of the 1^{--} still badly violate covariance, splitting the Lorentz multiplet and having asymmetrical dispersion. Since it is not yet behavingly covariantly overall, we do not attempt a detailed phenomenological analysis of the resulting wave functions. On the other hand, we are able to achieve a relatively symmetrical dispersion for the 0^{-+} state, with intercept $\mathcal{M}_\pi=171$ MeV and decay constant $f_\pi=132$ MeV, close to the experimental pion values. (The exact values would be obtainable with a sufficiently fine sweep of couplings.)

We checked that no Fock sectors are being artificially suppressed and that the truncation to no more than three links is not causing severe ''finite-volume'' effects from the maximum separation this imposes on anti-quark and quark. Table IV shows that the peak in the transverse spatial distribution of the 0^{-+} wave function is well-accomodated by the three-link cutoff (results are similar for the 1^{--}). However, the tail of the wave function at four and higher links may contain a significant total probability, which will affect ob-

TABLE III. Meson dispersion at the optimum couplings. π is the lightest 0^{-+} state, $\rho_{\pm,0}$ the lightest 1^- states with projections $\mathcal{J}_3=\pm 1,0$.

State	Mass (MeV)	c
π	171	1.02
ρ_0	828	0.99
ρ_+	457	1.04
ρ_-	457	0.76

TABLE IV. Probability for finding a certain number of links in the 0^{-+} state. The extrapolation errors in parentheses are from a $1/K$ extrapolation.

No Links	0	1	2	3
Probability	0.097(14)	0.661(10)	0.150(8)	0.087(2)

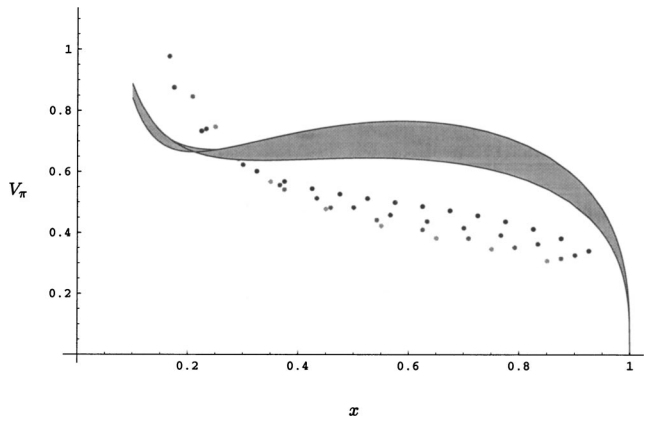

FIG. 6. Distribution function for DLCQ cutoffs $K=10,12,15,20$, darker data points meaning larger K. $K\to\infty$ extrapolated curve lies in the shaded region.

servables sensitive to very small transverse momenta. Therefore, in this paper we restrict our attention to observables integrated over all available transverse momenta. Indeed, when varying the Tamm-Dancoff cutoff above three links, we find very little change in the observables investigated below.

IV. PION OBSERVABLES

A. Valence quark structure function

The valence quark distribution function is defined as

$$V(x)=\sum_{h,h'}|\psi_{hh'}(x,1-x)|^2+\sum_{\lambda}\sum_{h,h'}\int_0^{1-x}dy|\psi_{h(\lambda)h'}(x,y,1-x-y)|^2+\sum_{\lambda,\rho}\sum_{h,h'}\int_0^{1-x}dy\int_0^{1-x-y}dz\times|\psi_{h(\lambda\rho)h'}(x,y,z,1-x-y-z)|^2+\cdots. \tag{30}$$

It is the probability for a quark to carry light-cone momentum fraction x. The result we find for $V(x)$ on the transverse lattice in the three-link truncation is shown in Fig. 6. The raw (discrete) DLCQ data for $K=10$, 12, 15, 20 are displayed together with an extrapolation to $K\to\infty$. To produce this, at each K data is fit to the momentum distribution form

$$xV(x)=(1-x)^\beta x^\alpha(a+b\sqrt{x}+cx). \tag{31}$$

We note that the simple form $x^\alpha(1-x)^\beta$, used to parameterize early experimental data, is not sufficient to fit our result. It is necessary to drop the $x=1/2K$ and $x=1-1/2K$ points from this analysis since they do not join smoothly to the rest of the distribution. This is because end point data are prone to artifacts resulting from the vanishing of some of the interactions in Table I. The smooth curves at each K are then extrapolated pointwise, by a (good) fit to a quadratic in $1/K$, for a large set of values in the interval $0.1<x<0.9$. The gray region represents the uncertainty from the extrapolation only.

The extrapolated data fits the form (31) with $\beta=0.33(2)$, $\alpha=0.3(1)$, $a=0.33(3)$, $b=-1.1(2)$, $c=2.0(3)$. The errors are from the extrapolation only. Bearing in mind that the extrapolation is based on fits to data that do not cover the end point regions, the true errors on α and β are likely to be much larger. From the first moment $\langle xV_\pi\rangle=\int_0^1 xV_\pi(x)dx$, we find that 32% of meson light-cone momentum is carried by the quarks, with the same carried by the anti-quarks. In the range $0.1<x<0.9$, over which there is some measure of control, the result for V_π is reminiscent of the constant $V_\pi=1$ distribution resulting from the chiral limit of chiral quark models [16]. However, because of the rapid rise at small x, which is expected on general grounds from Regge-type behavior [17], the flat part of the distribution is at $V\sim0.7$. Moreover, in the chiral quark models, all the light-cone momentum is carried by quarks, while here 36% is carried by the link fields representing gluonic degrees of freedom.

In order to compare with experimental data, one must address the transverse resolution scale. A well-defined transverse resolution scale is associated with $V(x)$ above, namely, the transverse lattice spacing a. If we were to repeat the calculation at a different a, one would expect to see an evolution of V as a result of the changing wave functions. In practice, the current transverse lattice method is only able to explore a small window in a—small enough to suppress discretization errors but large enough for the use of massive disordered link fields—which is too small to reliably quantify such evolution. Perturbative evolution equations typically use a different renormalization scheme, so there is no simple match between scales used in each scheme. In principle, there are wave function renormalisation constants of $O(1)$ that relate lattice operators to continuum operators, but these are also usually evaluated perturbatively. For example, in Euclidean lattice QCD [18], this has been done for moments of the operator expectation giving rise to V, since sufficiently fine lattices can be used to employ schemes matched to perturbation theory. Most low-energy effective theories for QCD, such as QCD sum rules [19,20], chiral quark models [16,21], and truncated Dyson-Schwinger equations [22], must resort to another method when attempting to compare with experimental data at higher resolution scales. The scale for input to perturbative evolution equations is fixed by matching one experimental datum; for example, the first moment of V. This is the procedure we will employ here for the color-dielectric tranverse lattice also, i.e. bare lattice operators are used, but with a resolution scale fixed once and for all by matching one experimental datum.

If we demand that $\langle xV_\pi\rangle\approx0.21$ at a scale of 2 GeV, as suggested by the analysis of E615 and NA10 pion-nucleon Drell-Yan data by Sutton *et al.* [23] for the valence quark distribution, then the scale associated to our result, if it were used as input for leading order non-singlet evolution, is $\mu\approx500$ MeV; this is reasonable given that $a^{-1}=300$ MeV. In Fig. 7 we show our result for $xV_\pi(x)$ evolved to 6.6 GeV and compared with the raw data for the valence distribution deduced by E615 [24] by combining data over scales 4-8.5 GeV. For completeness, we also show fits to $xV=x^\alpha(1-x)^\beta$ produced by earlier experiments NA10 [25] and NA3 [26]. In the valence region $x>0.5$, our result agrees with the most recent experiment, which claims a more accurate rep-

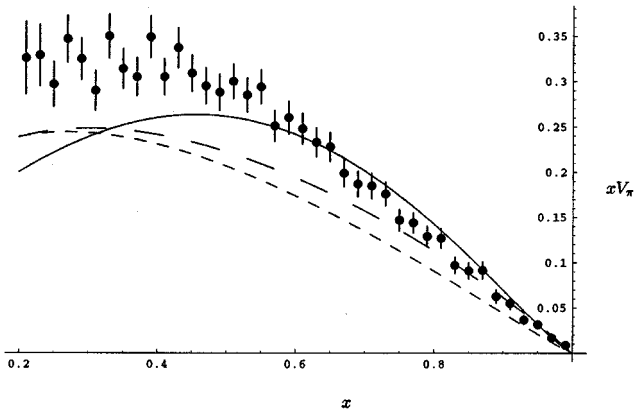

FIG. 7. Valence distribution functions (times x) compared to pion-nucleon Drell-Yan data. Solid line: transverse lattice result evolved at 6.6 GeV. Data points: E615 experiment [24]. Short-dashed line: NA10 experiment fit to $x^\alpha(1-x)^\beta$ form [25]. Long-dashed line: NA3 experiment fit to $x^\alpha(1-x)^\beta$ form [26].

resentation at large x. At smaller x there is not much agreement, either between experiments or with our result. This is hardly surprising given the sensitivity of this region to assumptions about the sea quarks or their measurement. In fact, our calculation contains no sea quarks since it is at large N_c. The recently discovered enhancement of initial-state interactions [27] is also expected to be most significant at small x, throwing into doubt the simple connection between light-cone probabilities and the Drell-Yan cross section [28]. It is obviously desirable to have data on V_π from sources other than the Drell-Yan process. This is also important from the theoretical perspective, given that the current Dyson-Schwinger approach predicts a completely different shape for the pion distribution function [29].

B. Distribution amplitude

The distribution amplitude (in $A_- = 0$ gauge) for the pion is defined by

$$\langle 0|\overline{\Psi}(z)\gamma^\mu\gamma_5\Psi(0)|\psi_\pi(P^\mu)\rangle\Big|_{z^2=0} = f_\pi P^\mu \int_0^1 e^{ix(z\cdot P)}\phi_\pi(x)dx, \tag{32}$$

with the normalization condition

$$\int_0^1 \phi_\pi(x) = 1. \tag{33}$$

If the quark field correlator is to be evaluated at equal light-cone time, $z^+ = 0$, then $\mathbf{z} = 0$ and z^- is arbitrary. This then measures the amplitude for zero transverse separation of quarks in the meson light-cone wave function. For the transverse lattice one finds

$$\psi_{+-}(x,1-x) = \frac{f_\pi}{2}\sqrt{\frac{\pi}{N_c}}\phi_\pi(x) \tag{34}$$

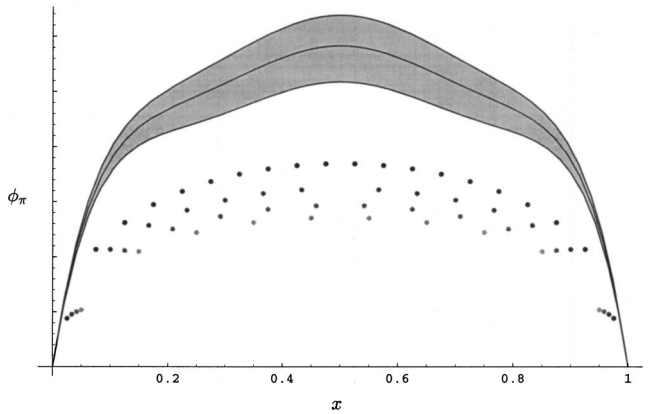

FIG. 8. Distribution amplitude for DLCQ cutoffs $K = 10,12,15,20$, darker data points meaning larger K. $K \to \infty$ extrapolated curve lies in the shaded region.

from the γ^+ component of Eq. (32). Figure 8 shows our results for the distribution amplitude at various K and extrapolated to $K = \infty$ in a three-link truncation. The raw (discrete) DLCQ data has been fit at each K to the first few terms of the conformal expansion [30,31]

$$\phi_\pi(x) = 6x(1-x)\{1 + a_2 C_2^{3/2}(1-2x) + a_4 C_4^{3/2}(1-2x)\}. \tag{35}$$

An extrapolation of the coefficients with $A + B/K + C/K^2$ yields $a_2 = 0.15(2)$, $a_4 = 0.04(1)$, confirming that truncation of the conformal expansion is justified. The same values are obtained if the fit curves at each K are pointwise extrapolated and then refit to Eq. (35). Finally, the result is insensitive to whether the $x = 1/2K$ and $x = 1 - 1/2K$ end points are included in the fit or not, so we have shown them in Fig. 8 also.

The distribution amplitude is indirectly accessible through the pion transition form factor $F_{\pi\gamma^*\gamma}(Q^2)$ measured at CLEO [32]. A perturbative QCD analysis relates this to the inverse moment, up to radiative corrections Δ,

$$\frac{3Q^2}{4\pi}F_{\gamma^*\gamma\pi} = \int_0^1 \frac{\phi_\pi(x)}{x} + \Delta = 3(1 + a_2 + a_4) + \Delta. \tag{36}$$

An analysis of the data in Ref. [33] extracted $a_2 + a_4 = 0.05 \pm 0.07$ at scale 2.4 GeV, taking into account next-to-leading order corrections $O(\alpha_s)$ in Δ. If we assume, following the structure function analysis, a transverse resolution scale 0.5 GeV for the transverse lattice result, when evolved to 2.4 GeV by the 1-loop evolution equations we find $a_2 = 0.07(1)$, $a_4 = 0.01(1)$ including only DLCQ errors. Although our result seems consistent with experiment, a couple of comments are necessary. The inverse moment is highly sensitive to the end point regions of ϕ_π, which are not well covered by the extrapolation of the DLCQ transverse lattice result. Also, the leading radiative corrections in Δ are large $\sim 20\%$, so one might ask about higher order corrections. The reader is referred to Refs. [16,34] for a more detailed review of the various theoretical and experimental results relating to ϕ_π.

Diffractive dissociation on a nucleus $\pi+A\to A+$jets [35] has been used to measure a cross section related to ϕ_π. A number a theoretical analyses of that relation have recently been performed [36], which differ in their conclusions about the precise relationship. Our result, when evolved to the higher transverse momentum scale of the experiments, is consistent with any one of the analyses, being close to the asymptotic form $6x(1-x)$. We mention that our DLCQ transverse lattice result for ϕ_π is close to one previously obtained in a one-link truncation using very similar methods [8], although a_4 was not fit and the normalization f_π was completely wrong in that case. The same one-link truncation was investigated in Ref. [9] by using basis functions instead of DLCQ and a similar (but not identical) criteria for fixing the Hamiltonian couplings. That gave a distribution amplitude a little closer to the asymptotic form, although a value for a_2 was not extracted and no error estimate was given. Thus, we can say with some confidence that our result is neither the ''double-hump'' first found by Chernyak and Zhitnitsky [19] using (local) sum rules nor the ''narrow hump'' one would deduce from most of the Euclidean lattice measurements of the lowest moment of ϕ_π [37] (see however the very recent result [38]).

C. Quark helicity correlation

Although the pion spin is 0, it nevertheless contains a complicated spin structure. One measure of this is the quark helicity correlations

$$C^{\rm para}(x)=\sum_h |\psi_{hh}(x,1-x)|^2 + \sum_\lambda \sum_h \int_0^{1-x} dy |\psi_{h(\lambda)h}(x,y,1-x-y)|^2 + \sum_{\lambda,\rho} \sum_h \int_0^{1-x} dy \int_0^{1-x-y} \times dz |\psi_{h(\lambda\rho)h}(x,y,z,1-x-y-z)|^2+\cdots, \tag{37}$$

$$C^{\rm anti}(x)=\sum_h |\psi_{-hh}(x,1-x)|^2 + \sum_\lambda \sum_h \int_0^{1-x} dy |\psi_{-h(\lambda)h}(x,y,1-x-y)|^2 + \sum_{\lambda,\rho} \sum_h \int_0^{1-x} dy \int_0^{1-x-y} \times dz |\psi_{-h(\lambda\rho)h}(x,y,z,1-x-y-z)|^2+\cdots. \tag{38}$$

Because the light-cone wave function essentially represents particles in an infinite-momentum frame, even massive particles have their spins aligned either parallel or anti-parallel to the ''fast'' x^3 direction in such a framework. The helicity correlations measure the probability for a quark to have light-cone momentum fraction x and helicity either parallel or anti-parallel to that of the anti-quark. Therefore, the sum is normalized to one (when integrated over x). These functions are plotted in Fig. 9. We estimate that

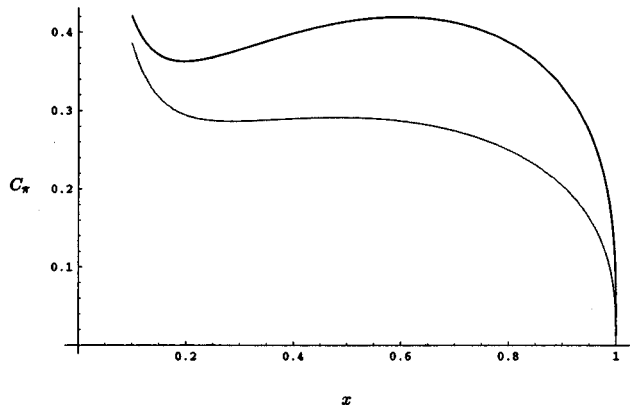

FIG. 9. Extrapolated quark helicity correlation function: black for anti-parallel helicities $C_\pi^{\rm anti}$; gray for parallel helicities $C_\pi^{\rm para}$.

$$\int_0^1 C_\pi^{\rm para} dx \sim 0.45. \tag{39}$$

Therefore, one is almost equally likely to find quark helicities aligned as anti-aligned. This is not necessarily inconsistent with the quark model picture of anti-parallel quark spins in a pion, since that model treats the glue as a non-relativistic potential. In a relativistic treatment, the gluonic degrees of freedom will carry some portion of the hadron momentum and helicity.

V. CONCLUSIONS

We have extended coarse transverse lattice calculations for mesons to physically realistic cutoffs on the anti-quark—quark separation. A general light-cone Hamiltonian in the large N_c limit was expanded in powers of dynamical fields and we studied a truncation of that color-dielectric expansion. This included all possible cubic terms and most of the quartic terms. By optimizing Lorentz covariance of glueball, heavy-source and meson bound states, the remaining freedom in the couplings in the Hamiltonian was reduced. By studying other symmetries, such as parity and chirality, it may be possible to constrain them further. In this paper, we performed a phenomenological calculation by fixing the remaining freedom in the couplings to best fit $\sqrt{\sigma}$, $\mathcal{M}_\pi$, $\mathcal{M}_\rho$, and f_π (two of these are parameters of the first-principles QCD).

The lightest meson bound state has the quantum numbers of the pion and exhibits a reasonably covariant lightcone wave function. Comparing the predictions of this wave function with various experimentally measured observables for the pion, we find consistency in the regions insensitive to sea quarks. New observables, which in principle can be extracted from a higher twist analysis of experiments, follow from the multiparton correlations in the light-cone wave function. As

an example, we computed the anti-quark—quark helicity correlation, suggesting that correlation is almost equally as likely as anti-correlation in the pion. Because the tail of the wave function in the transverse direction is still truncated in our calculation, we did not compute observables sensitive to small transverse momentum. Nevertheless, it would be interesting to look at the general features of the skewed parton distributions for intermediate momentum transfers, since little hard information is available for these important observables. It should be straightforward to extend the calculations to strange mesons and heavy-light mesons.

There are still some shortcomings in the calculation. The bound state most naturally identified with the rho is not yet behaving covariantly. Our optimization of chiral symmetry could be considerably improved. Given the close connection of Lorentz and chiral symmetry on the lattice, we believe that these problems are related. In particular, higher-order terms in the color-dielectric expansion can fulfill a dual role to improve both these symmetries.

ACKNOWLEDGMENTS

The work of S.D. was supported by PPARC grants GR/LO3965 and PPA/G/O/2000/00448. B.v.d.S. was supported by the Research Corporation. We would like to thank Geneva College undergraduates E. M. Watson and J. Bratt for help with developing the numerical code.

APPENDIX: CHIRAL SYMMETRY

The lattice Lagrangian (3) explicitly breaks chiral symmetry

$$\Psi \to e^{-i\theta\gamma_5}\Psi, \tag{A1}$$

through the bare mass-term μ_f and Wilson term κ_s. The standard test for this at the hadron level is PCAC

$$\langle 0|\partial_\mu A^\mu|\psi_\pi\rangle = f_\pi \mathcal{M}_\pi^2, \tag{A2}$$

where A_μ is the axial current. Without knowing the precise form of A_μ, one can use $\mathcal{M}_\pi$ to quantify the amount of explicit chiral symmetry breaking relative to other scales, such as the pure-QCD mass gap or the spontaneous chiral symmetry breaking scale given by the difference between $\mathcal{M}_\pi$ and masses of other light mesons. The result (A2) relies on exact Lorentz covariance, which is not present on the transverse lattice. In fact, in the calculation performed in this paper, the splitting of the ρ Lorentz multiplet is of comparable strength to the π-ρ splitting. This suggests that explicit chiral symmetry breaking effects are larger than $\mathcal{M}_\pi$ would suggest, perhaps of the same order as spontaneous chiral symmetry breaking effects.

Explicit chiral symmetry breaking could in principle be tested more directly. There is a $(1+1)$-dimensional Noether ''vector'' current

$$j^\alpha = \sum_{\mathbf{x}} \bar{\Psi}(\mathbf{x})\gamma^\alpha\Psi(\mathbf{x}) \tag{A3}$$

that is conserved under the equations of motion, i.e., $\partial_\alpha j^\alpha = 0$, and a corresponding chiral current

$$j_5^\alpha = \sum_{\mathbf{x}} \bar{\Psi}(\mathbf{x})\gamma^\alpha\gamma_5\Psi(\mathbf{x}) \tag{A4}$$

for which we find

$$\partial_\alpha j_5^\alpha = 2\mu_f^2 \sum_{\mathbf{x},h} hF_h^\dagger(\mathbf{x})\frac{1}{\partial_-}F_h(\mathbf{x}), \tag{A5}$$

where F_h is defined in Eq. (8). One might then use a matrix element such as

$$\langle 0|\partial_\alpha j_5^\alpha|\psi_\pi\rangle \tag{A6}$$

to quantify explicit chiral symmetry violation, minimizing it by finite renormalizations of couplings, since the vanishing of Eq. (A6) is a necessary condition for conservation of the four-dimensional axial current. There are a few difficulties that must be overcome before this would be practical however. The expression (A5) has a normal-ordering ambiguity similar to the Hamiltonian. Moreover, it is much more computationally expensive to perform symmetry tests with eigenfunctions rather than eigenvalues. On a coarse lattice, the chiral symmetry breaking couplings are also strongly constrained away from zero by Lorentz covariance; for example, κ_s is needed to avoid fermion doubling [7]. It would therefore be desirable to have further independent chiral symmetry breaking couplings in Hamiltonian to tune.

Natural candidates are the transverse lattice versions of the Sheikholeslami-Wohlert (SW) terms [39], $\bar{\Psi}\sigma^{\mu\nu}F_{\mu\nu}\Psi$. In Euclidean lattice gauge theory they can be tuned to remove $O(a)$ contributions to chiral current non-conservation [40]. On a transverse lattice they become

$$\bar{\Psi}(\mathbf{x})\sigma^{rs}[M_r(\mathbf{x})M_s(\mathbf{x}+a\hat{\mathbf{r}}) - M_s(\mathbf{x})M_r(\mathbf{x}+a\hat{\mathbf{s}})]\Psi(\mathbf{x}+a\hat{\mathbf{r}}+a\hat{\mathbf{s}}), \tag{A7}$$

$$\bar{\Psi}(\mathbf{x})\sigma^{+-}F_{+-}\Psi(\mathbf{x}). \tag{A8}$$

In the dimensional counting classification of Euclidean lattice quark operators, SW terms occur along with Wilson terms at dimension five. On the coarse transverse lattice their significance is not so obvious, since they enter at higher orders of the color-dielectric expansion in powers of dynamical fields. Terms of the form (A7), (A8) in the Lagrangian give rise to coupled constraint equations of motion for non-dynamical fields. If solved order by order in dynamical fields, they give rise to new interactions in the gauge-fixed light-cone Hamiltonian starting at orders is u^4, u^2M^2. Of particular interest are interactions generated at order u^2M^3 and u^4M that flip the helicity h of quarks. Interactions of this kind carry the spontaneous chiral symmetry breaking effects in effective light-cone Hamiltonians [41]; the $m_f k_a$ and $k_s k_a$ terms performed this function in Eq. (26).

[1] S.J. Brodsky, Acta Phys. Pol. B **32**, 4013 (2001); S.J. Brodsky, H.-C. Pauli, and S. Pinsky, Phys. Rep. **301**, 299 (1998).
[2] W.A. Bardeen and R.B. Pearson, Phys. Rev. D **14**, 547 (1976); W.A. Bardeen, R.B. Pearson, and E. Rabinovici, *ibid.* **21**, 1037 (1980).
[3] M. Burkardt and S. Dalley, Prog. Part. Nucl. Phys. **48**, 317 (2002).
[4] P.A. Griffin, Nucl. Phys. **B139**, 270 (1992).
[5] S. Dalley and B. van de Sande, Phys. Rev. D **56**, 7917 (1997); **59**, 065008 (1999); Phys. Rev. Lett. **82**, 1088 (1999); Phys. Rev. D **62**, 014507 (2000); **63**, 076004 (2001).
[6] M. Burkardt and B. Klindworth, Phys. Rev. D **55**, 1001 (1997).
[7] M. Burkardt and H. El-Khozondar, Phys. Rev. D **60**, 054504 (1999).
[8] S. Dalley, Phys. Rev. D **64**, 036006 (2001)
[9] M. Burkardt and S.K. Seal, Phys. Rev. D **64**, 111501(R) (2001); **65**, 034501 (2002).
[10] H.-C. Pauli and S.J. Brodsky, Phys. Rev. D **32**, 1993 (1985); **32**, 2001 (1985).
[11] A. Casher, Phys. Rev. D **14**, 452 (1976); T. Maskawa and K. Yamawaki, Prog. Theor. Phys. **56**, 270 (1976); C. Thorn, Phys. Lett. **70B**, 77 (1977).
[12] F. Antonuccio and S. Dalley, Phys. Lett. B **376**, 154 (1996); Nucl. Phys. **B461**, 275 (1996).
[13] G. 't Hooft, Nucl. Phys. **B75**, 461 (1974).
[14] M. Burkardt, Phys. Rev. D **57**, 1136 (1998).
[15] R. Perry and A. Harindranath, Phys. Rev. D **43**, 4051 (1991).
[16] E. Ruiz Arriola, in *Lectures at 42nd Cracow School of Theoretical Physics on Pion Structure at High and Low Energies in Chiral Quark Models*, Zakopane, Poland, 2002 [Acta Phys. Pol. B **33**, 4443 (2002)].
[17] F. Antonuccio, S.J. Brodsky, and S. Dalley, Phys. Lett. B **412**, 104 (1997).
[18] QCDSF Collaboration, S. Capitani *et al.*, Nucl. Phys. B (Proc. Suppl.) **106A**, 299 (2002); C. Best *et al.*, Phys. Rev. D **56**, 2743 (1997).
[19] V.L. Chernyak and A.R. Zhitnitsky, Phys. Rep. **112**, 173 (1984).
[20] S.V. Mikhailov and A.V. Radyushkin, Phys. Rev. D **45**, 1754 (1992).
[21] T. Heinzl, hep-th/9812190; K. Itakura and S. Maedan, Phys. Rev. D **62**, 105016 (2000).
[22] M.B. Hecht, C.D. Roberts, and S.M. Schmidt, Phys. Rev. C **63**, 025213 (2001).
[23] P.J. Sutton *et al.*, Phys. Rev. D **45**, 2349 (1992).
[24] E615 Collaboration, J.S. Conway *et al.*, Phys. Rev. D **39**, 92 (1989).
[25] NA10 Collaboration, B. Betev *et al.*, Z. Phys. C **28**, 15 (1985).
[26] NA3 Collaboration, J. Badier *et al.*, Z. Phys. C **18**, 281 (1983).
[27] S.J. Brodsky *et al.*, Phys. Rev. D **65**, 114025 (2002).
[28] S.D. Drell and T.M. Yan, Phys. Rev. Lett. **24**, 181 (1970).
[29] C.D. Roberts, Nucl. Phys. B (Proc. Suppl.) **108A**, 227 (2002).
[30] G.P. Lepage and S.J. Brodsky, Phys. Lett. **87B**, 359 (1979); **22B**, 2157 (1980).
[31] A.V. Efremov and A.V. Radyushkin, Phys. Lett. **94B**, 245 (1980); Theor. Math. Phys. **42**, 97 (1980).
[32] CLEO Collaboration, J. Gronberg *et al.*, Phys. Rev. D **57**, 33 (1998).
[33] A. Schmedding and O. Yakovlev, Phys. Rev. D **62**, 116002 (2000).
[34] A.P. Bakulev, S.V. Mikhailov, and N.G. Stefanis, Phys. Lett. B **508**, 279 (2001).
[35] E791 Collaboration, E.M. Aitala *et al.*, Phys. Rev. Lett. **86**, 4768 (2001).
[36] L. Frankfurt, G.A. Miller, and M. Strikman, Phys. Rev. D **65**, 094015 (2002); V.M. Braun, D.Yu. Ivanov, A. Schafer, and L. Szymanowski, Phys. Lett. B **509**, 43 (2001); Nucl. Phys. **B638**, 111 (2002); V.L. Chernyak and A.G. Grozin, Phys. Lett. B **517**, 119 (2001).
[37] L. Del Debbio *et al.*, Nucl. Phys. B (Proc. Suppl.) **83A**, 235 (2000).
[38] L. Del Debbio *et al.*, "The Second Moment of the Pion Light Cone Wave Function," in Proceedings of the International Conference on Lattice 2002, hep-lat/0211037.
[39] B. Sheikholeslami and R. Wohlert, Nucl. Phys. **B259**, 572 (1985).
[40] M. Lüscher *et al.*, Nucl. Phys. B (Proc. Suppl.) **53A**, 905 (1997).
[41] K.G. Wilson *et al.*, Phys. Rev. D **49**, 6720 (1994).